Monthly Notices
of the
ROYAL ASTRONOMICAL SOCIETY

MNRAS **450,** 3665–3674 (2015) doi:10.1093/mnras/stu2505

CoMaLit – III. Literature catalogues of weak lensing clusters of galaxies (LC^2)

Mauro Sereno★

Dipartimento di Fisica e Astronomia, Università di Bologna, viale Berti Pichat 6/2, 40127 Bologna, Italia

Accepted 2014 November 24. Received 2014 November 11; in original form 2014 September 17

ABSTRACT

The measurement of the mass of clusters of galaxies is crucial for their use in cosmology and astrophysics. Masses can be efficiently determined with weak lensing (WL) analyses. I compiled literature catalogues of WL clusters (LC^2). Cluster identifiers, coordinates, and redshifts have been standardized. WL masses were reported to over-densities of 2500, 500, 200, and to the virial one in the reference ΛCDM model. Duplicate entries were carefully handled. I produced three catalogues: LC^2-*single*, with 485 unique groups and clusters analysed with the single-halo model; LC^2-*substructure*, listing substructures in complex systems; LC^2-*all*, listing all the 822 WL masses found in the literature. The catalogues and future updates are publicly available at http://pico.bo.astro.it/~sereno/CoMaLit/LC2/.

Key words: gravitational lensing: weak – catalogues – galaxies: clusters: general.

1 INTRODUCTION

Clusters of galaxies are at the crossroad between cosmology and astrophysics. They are laboratories to study the physics of baryons and dark matter at large scales in bound objects (Voit 2005; Pratt et al. 2009; Arnaud et al. 2010; Giodini et al. 2013). Cosmological parameters can be measured with cluster abundances and the observed growth of massive galaxy clusters (Mantz et al. 2010; Planck Collaboration et al. 2014), with gas fractions (Ettori et al. 2009), or lensing analyses (Sereno 2002; Jullo et al. 2010; Lubini et al. 2014). This requires precise and accurate measurements of the cluster masses.

Cluster properties that can be easily measured with ongoing and future large surveys (Laureijs et al. 2011), such as optical richness, X-ray luminosity and Sunyaev–Zel'dovich (SZ) flux, are going to be used as mass proxies. This relies on an accurate calibration through comparison with direct mass estimates (Andreon & Bergé 2012; Ettori 2013; Sereno & Ettori 2015a, hereafter CoMaLit-I; Sereno, Ettori & Moscardini 2014).

Weak lensing (WL) analyses provide one of the most well-regarded mass estimates (Bartelmann & Schneider 2001). The physics behind gravitational lensing is well understood. The shear distortions of the background galaxies trace the gravitational field of the matter distribution of the lens (Hoekstra et al. 2012; von der Linden et al. 2014; Umetsu et al. 2014).

Even if the WL estimate of the total projected mass along the line of sight is precise, the approximations that have to be used (spherical symmetry, smooth density distributions and no other contribution along the line of sight) to infer the three-dimensional mass may bias and scatter the results.

The main sources of uncertainty in WL mass estimates are due to triaxiality and substructures. The spherical assumption can bias the results for triaxial clusters pointing towards the observer, wherein lensing strengths are boosted and mass and concentration are overestimated, or for clusters elongated in the plane of the sky, wherein mass and concentration are, in contrast, underestimated (Oguri et al. 2005; Sereno 2007; Corless, King & Clowe 2009; Sereno, Jetzer & Lubini 2010; Sereno & Umetsu 2011; Sereno & Zitrin 2012).

Substructures in the cluster surroundings may dilute the tangential shear signal (Meneghetti et al. 2010; Giocoli et al. 2012, 2014). Significant mass underestimations can be caused by either massive sub-clumps just outside the virial radius (Meneghetti et al. 2010) or uncorrelated large-scale matter projections along the line of sight (Becker & Kravtsov 2011).

Numerical studies have quantified the extent to which bias and intrinsic scatter affect WL masses. Usual fitting procedures for the cluster tangential shear profiles can bias the mass down by ∼5–10 per cent with a scatter of ∼10–25 per cent (Meneghetti et al. 2010; Becker & Kravtsov 2011; Rasia et al. 2012). The exact value of the bias depends both on cluster mass and on radial survey range (Bahé, McCarthy & King 2012). The scatter should be less significant in optimally selected clusters either having regular morphology or living in substructure-poor environments (Rasia et al. 2012).

These theoretical predictions agree with recent measurements. Sereno & Ettori (2015a) determined an intrinsic scatter for WL masses of ∼15 per cent. The scatter was estimated by comparing WL to X-ray masses based on the hypothesis of hydrostatic equilibrium for a number of well-observed clusters from either the CLASH (Cluster Lensing And Supernova survey with Hubble, Postman et al.

★ E-mail: mauro.sereno@unibo.it

2012; Umetsu et al. 2014), the CCCP (Canadian Cluster Comparison Project, Hoekstra et al. 2012; Mahdavi et al. 2013), or the WtG (Weighing the Giants, von der Linden et al. 2014; Applegate et al. 2014) programmes.

An alternative and popular method to infer the cluster mass is based on the assumption that hydrostatic equilibrium holds between the intra-cluster medium and the gravitational potential. The cluster mass can then be recovered from observations of the X-ray temperature and surface brightness (LaRoque et al. 2006; Donahue et al. 2014). However, deviations from equilibrium or non-thermal contributions to the pressure are difficult to quantify and can bias the mass estimate to a larger extent than for WL masses (Rasia et al. 2012; CoMaLit-I).

Other methods to derive the cluster mass employ spectroscopic measurements of galaxy velocities, such as the caustic technique (Rines & Diaferio 2006), or approaches exploiting the Jeans equation (Lemze et al. 2009; Biviano et al. 2013). These methods require observations more expansive than photometric surveys and are mostly limited to low redshift haloes.

WL masses can be obtained up to high redshifts in the context of large photometric surveys, and they are nearly unbiased. They are supposedly the best mass estimators to calibrate other proxies.

In this paper, I re-elaborate in a standard form known WL mass estimates of galaxy clusters available in the literature. The typical information presented in WL studies is not standardized. A cluster can be named in different ways. Different conventions are employed for the reference cosmological model. The lens can be characterized in a number of ways. A quantitative analysis can provide either the total mass within an integration radius (which can be defined in several ways), or the total projected mass within an angular aperture (this is the quantity the lensing is most sensitive to), or the parameters characterizing the adopted mass profile.

I collected all the disparate WL measurements available in the literature in three meta-catalogues regularized to the same reference cosmology and to the same set of integration radii. The basic characteristics of these catalogues are the large number of objects (485 unique systems), and the standardized names, coordinates, redshifts and masses. References to the original analyses were reported for each cluster.

I compiled three catalogues: (i) LC^2-*single* lists the unique systems. Duplicate entries originating from overlaps between the input references were controlled and eliminated. The reported masses of either regular or complex clusters were obtained with a single-halo analysis. These are the most sensible masses to compare to other global properties, such as the SZ flux, the X-ray luminosity or the optical richness. (ii) LC^2-*substructure* lists the main and the secondary substructures of complex clusters, which were studied with a multiple-halo analysis. The mass of each component is reported individually. (iii) LC^2-*all* lists all the groups and clusters found in the literature. Repeated entries are included. LC^2-*single* and LC^2-*substructure* are subsamples of LC^2-*all*.

The catalogues are publicly available in electronic format and will be periodically updated.

In compiling the catalogues[1], I assumed a fiducial flat ΛCDM cosmology with density parameter $\Omega_{M0} = 0.3$, and Hubble constant $H_0 = 70\,\mathrm{km\,s^{-1}\,Mpc^{-1}}$.

This paper is the third in a series titled 'CoMaLit' (Comparing Masses in the Literature). In the first paper (CoMaLit-I), systematic differences in lensing and X-ray masses obtained from independent analyses were quantified and the overall level of bias and intrinsic scatter was assessed through Bayesian techniques. This formalism was later applied and developed in the second paper of the series (Sereno et al. 2015, hereafter CoMaLit-II) to calibrate the SZ flux estimated by the Planck satellite against mass proxies. The fourth paper (Sereno & Ettori 2015b, hereafter CoMaLit-IV)[2] studies the time evolution of the scaling relations.

The paper is structured as follows. In Section 2, I comment on qualities and drawbacks of meta-catalogues collected from the literature and on their use in astronomy. In Section 3, I review the various definitions of over-density and virial radii and I motivate the choice of the radii used for the catalogues. In Section 4, I summarize the properties of the most used mass density distributions to characterize the lens and I discuss how I standardized the estimates of the masses listed in the catalogues. Section 5 discusses the dependence of the WL mass estimates on the cosmological parameters and how they can be made uniform to a given reference cosmological model. In Section 6, I discuss how I assembled the catalogues from the various literature sources and how I identified the clusters. Section 7 presents the format of the catalogues. Final considerations are in Section 8.

2 ON META-CATALOGUES

The worthiness of coherently compiled meta-catalogues of clusters has been discussed in Piffaretti et al. (2011), who collected a large catalogue of clusters of galaxies detected by X-rays based on publicly available samples.

Specifically for the WL catalogues here presented, LC^2-*all* provides a panorama of the state of the art on WL clusters. It gives an overview of the published, publicly available WL analyses. It is a repository of references and a ready-to-use collection of the main properties (coordinates, redshift and mass) of the observed clusters.

Large, standardized catalogues can be used for cross-correlation with existing, ongoing or upcoming surveys at various wavelengths, such as SZ (Reichardt et al. 2013; Menanteau et al. 2013; Planck Collaboration et al. 2014), optical (Laureijs et al. 2011, Euclid) or X-ray surveys (Piffaretti et al. 2011, and references therein). The mass, in combination with the appropriate scaling laws, enables us to predict all the main properties of the clusters, such as the integrated SZ flux, the X-ray temperature, the optical richness and the velocity dispersion.

The largest public catalogues of massive WL clusters consist of a few dozens of objects (Shan et al. 2012; Mahdavi et al. 2013; Applegate et al. 2014; Umetsu et al. 2014). Clusters are not usually selected according to strict selection functions and some sort of arbitrariness can persist. The usual WL sample that can be found in the literature is then small but it is neither statistical nor complete. It can be worthwhile taking a different route, i.e. to consider a sample whose selection function is not known but that is as large as possible. A very large sample, no matter whether it was assembled in a heterogeneous way, can recover the actual physical trends we are looking for (Gott et al. 2001).

The LC^2 catalogues can be useful in the construction of better defined subsamples. The full sample of collected clusters is neither statistical nor complete. The reconstruction of the selection function of meta-catalogues is a nearly impossible task (Piffaretti et al. 2011). The individual selection functions of the subsamples are complex

[1] http://pico.bo.astro.it/~sereno/CoMaLit/LC2/

[2] Products of the CoMaLit series are publicly available at http://pico.bo.astro.it/~sereno/CoMaLit/.

and, in most cases, are not known or not available. However, suitable subsamples can be extracted for which the selection function can be approximated. These subsamples can be used to study scaling relations, the time evolution of structures and cosmography.

A large collection of clusters enables us to assess the reliability of the WL mass measurements (CoMaLit-I). The repeated entries in LC^2-*all* can be used to compare mass estimates from different analyses. Published uncertainties are often unable to account for the actual variance seen in sample pairs (Rozo et al. 2014; CoMaLit-I). The certain assessment of cluster masses is hindered by instrumental and methodological sources of errors, which may cause systematic uncertainties in data analysis (Rozo et al. 2014). The main sources of systematics in lensing analyses are due to selection and calibration problems. The selection and redshift measurement of background galaxies is a very difficult task, which has to be undertaken with accurate photometric redshifts and colour–colour selection methods (Medezinski et al. 2010; Gruen et al. 2014). A small calibration correction of the shear signal of the order of just a few per cent can produce a systematic error of ∼10 per cent in the estimate of the virial mass (Umetsu et al. 2014). Differences in WL mass estimates reported by different groups can be as large as ∼40 per cent (CoMaLit-I).

Even though the catalogues are presented in a uniform format, they are highly heterogeneous. The clusters were detected in a variety of ways within X-ray, optical, SZ or shear surveys. Some clusters were targeted because they are very peculiar objects, such as merging (Okabe & Umetsu 2008) or high redshift clusters (Jee et al. 2011). Some samples of clusters were assembled based on their known properties, such as their X-ray luminosity or regular X-ray morphology (Mahdavi et al. 2013; von der Linden et al. 2014; Umetsu et al. 2014). Others were observed in follow-up programmes of differently planned surveys, which significantly increased the number of studied lensing clusters and extended the observation range to lower mass objects (McInnes et al. 2009; Kettula et al. 2013). Some samples were shear selected (Shan et al. 2012).

On the positive side, systematic biases that affect some specific, small samples may average out in a heterogeneous and very large sample. The larger the sample, the smaller the biases due to the orientation of the clusters, to their internal structure and to the projection effect of large-scale structure. Due to the different finding techniques, biases plaguing lensing selected samples, such as the over-concentration problem and the orientation bias (Oguri & Blandford 2009; Meneghetti et al. 2011), are mitigated too. Projection effects are less severe for clusters detected by X-ray or SZ methods.

The different observational facilities and data analysis methods also increase the heterogeneous nature of the catalogue. Different solutions to instrumental and methodological sources of errors may cause systematic errors in the mass determination. The heterogeneity of the catalogues manifests both in the listed central estimates and the uncertainties. Masses are presented in a homogeneous way but they were not derived homogeneously among the original studies.

3 MASSES

Total masses of clusters within an over-dense region can be related to the virial mass. Most cluster properties are expected to be self-similar at those scales. There are several commonly used definitions of the virial radius. Over-densities can be measured either with respect to the critical density of the universe at the epoch of analysis ($\Delta_{\rm cr}$) or with respect to the mean density ($\Delta_{\rm m}$). For the compilation of the catalogue, I considered $\Delta = \Delta_{\rm cr}$, in terms of which important properties of galaxy clusters are universal (Diemer & Kravtsov 2015).

M_Δ denotes the mass within the radius r_Δ, which encloses a mean over-density of Δ times the critical density at the cluster redshift, $\rho_{\rm cr} = 3H(z)^2/(8\pi G)$; $H(z)$ is the Hubble parameter, which is dependent on redshift. By definition, M_Δ can be expressed as

$$M_\Delta = \frac{4\pi}{3}\Delta\rho_{\rm cr} r_\Delta^3. \quad (1)$$

Numerical simulations show that fixed over-densities are very useful for describing universal features of clusters and for studying the scaling relations (Tinker et al. 2008; Diemer & Kravtsov 2015). From the theoretical point of view, the virialized region of a cluster can be related to the solution for the collapse of top-hat perturbations. The viral over-density is then dependent on redshift and cosmology. To compute the virial radius, I adopted the approximate relation proposed by Bryan & Norman (1998), which is based on the spherical collapse model for a flat universe with cosmological constant:

$$\Delta_{\rm vir} \simeq 18\pi^2 + 82[\Omega_{\rm M}(z) - 1] - 39[\Omega_{\rm M}(z) - 1]^2. \quad (2)$$

WL studies probe the clusters on large radial scales. As integration radii, I considered the virial radius and r_{200}, which usually enclose most of the field of view covered by observations and are also well probed by SZ analyses; r_{500}, which still encloses a substantial fraction of the total virialized mass of the system and is usually the largest radius probed in X-ray observations; and r_{2500}, which is usually poorly constrained by WL alone but can still be useful in comparison with a detailed analysis of the cluster core, such as those based on current high-resolution X-ray observations or strong lensing investigations. Results for r_{2500} are mostly based on extrapolations and they may be unreliable without strong lensing constraints.

The critical surface density for lensing is defined as

$$\Sigma_{\rm cr} \equiv \frac{c^2\, D_{\rm s}}{4\pi G\, D_{\rm d}\, D_{\rm ds}}, \quad (3)$$

where $D_{\rm s}$, $D_{\rm d}$ and $D_{\rm ds}$ are the source, the lens and the lens–source angular diameter distances, respectively.

4 MASS PROFILES

Whenever the masses M_Δ were quoted in the original papers, I used them for the catalogues. If not, I had to extrapolate the quoted results based on the density profile adopted in the analysis. The Navarro–Frenk–White profile (Navarro, Frenk & White 1996, NFW), and the singular isothermal sphere (SIS) are the standard parametric models used in lensing analyses to characterize the deflector.

Alternatively, some works quote only the total projected mass in an angular aperture. This may be the case for combined strong and WL analyses or of free-form modelling. In these cases, I extrapolated the results by adopting a NFW model.

4.1 Navarro–Frenk–White profile

Dark matter haloes are successfully described as NFW density profiles (Navarro et al. 1996; Jing & Suto 2002). The 3D density distribution follows

$$\rho_{\rm NFW} = \frac{\rho_{\rm s}}{(r/r_{\rm s})(1 + r/r_{\rm s})^2}, \quad (4)$$

where r_s is the scale radius. The mass enclosed at radius r is

$$M_{\rm NFW}(<r) = 4\pi\rho_s r_s^3 F_{\rm NFW}(r_s/r), \quad (5)$$

where

$$F_{\rm NFW}(x) = x^3\left[\ln(1+x^{-1}) - (1+x)^{-1}\right]. \quad (6)$$

The NFW model is characterized by two parameters. They can be ρ_s and r_s, or the mass M_Δ and the concentration, $c_\Delta \equiv r_\Delta/r_s$. The conversion relations are simple. From the definition of concentration and equation (5),

$$r_s = r_\Delta/c_\Delta \quad (7)$$

and

$$\rho_s = \frac{\Delta}{3}\frac{1}{F_{\rm NFW}(1/c_\Delta)}\rho_{\rm cr}. \quad (8)$$

The general conversion from a mass at an arbitrary over-density, Δ_1, to a second one, Δ_2, was derived in Hu & Kravtsov (2003). By writing the parameters r_s and ρ_s in terms of two different over-densities through equations (7) and (8) and equating the expressions, we obtain

$$F_{\rm NFW}\left(\frac{1}{c_{\Delta_2}}\right) = \frac{\Delta_2}{\Delta_1}F_{\rm NFW}\left(\frac{1}{c_{\Delta_1}}\right), \quad (9)$$

$$M_{\Delta_2} = \frac{\Delta_2}{\Delta_1}\left(\frac{c_{\Delta_2}}{c_{\Delta_1}}\right)^3 M_{\Delta_1}. \quad (10)$$

The conversion involves the inversion of the function $F_{\rm NFW}(x)$.

Equations (9) and (10) can also be rewritten to derive the concentrations given two integrated masses, M_{Δ_1} and M_{Δ_2},

$$F_{\rm NFW}\left(\frac{1}{c_{\Delta_1}}\left(\frac{\Delta_2 M_{\Delta_1}}{\Delta_1 M_{\Delta_2}}\right)^{1/3}\right) = \frac{\Delta_2}{\Delta_1}F_{\rm NFW}\left(\frac{1}{c_{\Delta_1}}\right); \quad (11)$$

given two masses and one concentration, the remaining concentration can be obtained as

$$c_{\Delta_2} = c_{\Delta_1}\left(\frac{\Delta_1 M_{\Delta_2}}{\Delta_2 M_{\Delta_1}}\right)^{1/3}. \quad (12)$$

An additional relation has to be used to constrain the NFW profile if only one parameter is known. *N*-body simulations have proved that mass and concentration are related (Neto et al. 2007; Gao et al. 2008; Duffy et al. 2008; Prada et al. 2012; Dutton & Macciò 2014; Diemer & Kravtsov 2015). In limited ranges, the dependence of the halo concentration on mass and redshift can be adequately described by a power law,

$$c_{200} = A(M_{200}/M_{\rm pivot})^B(1+z)^C. \quad (13)$$

Simulations show that concentrations are scattered about the median relation. The scatter is approximately log-normal and it is of the order of ∼30 per cent (Duffy et al. 2008; Bhattacharya et al. 2013). Whereas different studies agree on the functional form of the relation (Diemer & Kravtsov 2015) and on the level of scatter, some disagreement as large as ∼50 per cent is still present for the overall normalization of the relation (Prada et al. 2012).

On the observational side, the concentration estimated with WL studies can differ from the intrinsic one due to uncorrelated or correlated large-scale structure, baryonic physics and, mainly, triaxiality and orientation of the halo ellipsoid with respect to the line of sight (Bahé et al. 2012; Giocoli et al. 2014).

If only one parameter is reported in the analysis, I broke the degeneracy in the mass profile by adopting the relation in equation (13) with $A = 5.71$, $B = -0.084$ and $C = -0.47$ for a pivotal mass $M_{\rm pivot} = 2\times10^{12}\,{\rm M}_\odot\,h^{-1}$ (Duffy et al. 2008). Uncertainties and scatter can affect the estimation of the extrapolated masses when the concentration is determined with a given mass–concentration relation. A deviation of the order of ∼30 per cent from the median c_{200} in a large mass ($10^{14}\,{\rm M}_\odot \lesssim M_{200} \lesssim 10^{15}\,{\rm M}_\odot$) and redshift ($z \lesssim 1$) range causes an analogue deviation for the estimate of M_{500} of the order of ∼20–30 per cent. On the other hand, the estimate of M_{200} from the analysis of the shear profile depends weakly on the assumed concentration (Applegate et al. 2014).

Some analyses quote only the projected mass within an aperture radius. The total projected mass for a NFW lens can be expressed as

$$M^{\rm cyl}_{\rm NFW}(<R) = 4\pi\rho_s r_s^3\left\{2\frac{\mathrm{arctanhh}\left|\frac{1-x}{1+x}\right|}{\sqrt{|1-x^2|}} + \ln\left(\frac{x}{2}\right)\right\}, \quad (14)$$

where x is the dimensionless projected radius, $x \equiv R/r_s$, and arctanhh = arctanh (arctan) if $x < (>)\,1$. If only the mass within a cylinder, $M^{\rm cyl}_{\rm obs}$, is provided, the mass M_Δ can be derived by inverting

$$M^{\rm cyl}_{\rm NFW}(R_{\rm obs}; M_\Delta, c_\Delta(M_\Delta)) = M^{\rm cyl}_{\rm obs}, \quad (15)$$

where $c_\Delta(M_\Delta)$ can be expressed as in equation (13).

4.2 Singular isothermal sphere

An alternative mass profile is provided by the singular isothermal sphere (Turner, Ostriker & Gott 1984), whose density profile is

$$\rho_{\rm SIS} = \frac{1}{2\pi}\frac{\sigma^2_{\rm SIS}}{G}\frac{1}{r^2}. \quad (16)$$

This model was the standard for lens profiles before being supplanted by the NFW model. The total mass within a spherical radius is

$$M_{\rm SIS}(<r) = \frac{2\sigma^2_{\rm SIS}}{G}r. \quad (17)$$

It follows that

$$r_\Delta = \frac{2\sigma^2_{\rm SIS}}{H(z)\sqrt{\Delta}} \quad (18)$$

and

$$M_\Delta = \frac{4\sigma^3_{\rm SIS}}{GH(z)\sqrt{\Delta}}. \quad (19)$$

5 COSMOLOGICAL PARAMETERS

Lensing mass estimates depend on the assumed cosmological model. If necessary, they were rescaled to the reference cosmological model, i.e. a flat ΛCDM cosmology with density parameter $\Omega_{\rm M0} = 0.3$, and Hubble constant $H_0 = 70\,{\rm km\,s^{-1}\,Mpc^{-1}}$.

The lensing 3D mass within a radius $r = D_{\rm d}\theta$, where θ is the angular radius, scales as (CoMaLit-I)

$$M^{\rm WL} \propto \Sigma_{\rm cr}D_{\rm d}^2\theta_{\rm E}\,\theta\,f(\theta), \quad (20)$$

where $\theta_{\rm E}$ is the angular Einstein radius. The function $f(\theta) \sim \theta^{\delta\gamma}$ quantifies the deviation of the mass profile from the isothermal case.

By equating equations (1) and (20) at $\theta_\Delta(= r_\Delta/D_{\rm d})$, we obtain

$$M^{\rm WL}_\Delta \propto D_{\rm d}^{-\frac{3\delta\gamma}{2-\delta\gamma}}\left(\frac{D_{\rm ds}}{D_{\rm s}}\right)^{-\frac{3}{2-\delta\gamma}}H(z)^{-\frac{1+\delta\gamma}{1-\delta\gamma/2}}. \quad (21)$$

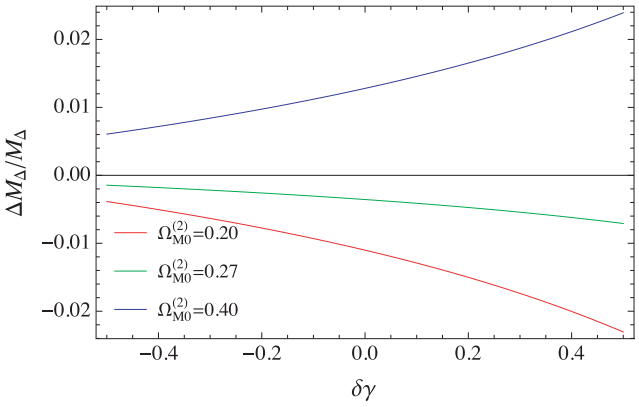

Figure 1. Relative variation of the estimated WL mass within a fixed over-density, M_Δ, as a function of the slope $\delta\gamma$ for different (flat) cosmological models with respect to the standard ΛCDM model with $\Omega_{M0} = 0.3$. The lens redshift is $z_d = 0.3$; the background galaxies are at $z_s = 1.0$. The red, green and blue lines refer to flat ΛCDM models with Ω_{M0} =0.20, 0.27 and 0.40, respectively.

Equation (21) holds for a fixed over-density, whereas the viral over-density depends on the cosmological parameters. For the virial mass,

$$M_{\rm vir}^{\rm WL} \propto \Delta_{\rm vir}^{-\frac{1+\delta\gamma}{2-\delta\gamma}} D_{\rm d}^{-\frac{3\delta\gamma}{2-\delta\gamma}} \left(\frac{D_{\rm ds}}{D_{\rm s}}\right)^{-\frac{3}{2-\delta\gamma}} H(z)^{-\frac{1+\delta\gamma}{1-\delta\gamma/2}}, \quad (22)$$

where $\Delta_{\rm vir}$ is a function of the redshift-dependent cosmological density; see equation (2).

The dependence on the cosmological parameters is usually small. The variation is $\lesssim$2 per cent for a large range of mass profiles and cosmological models; see Fig. 1.

The condition $\delta\gamma = 0$ is strictly verified only for the singular isothermal profile but it provides a good approximation in general. Let us consider as a typical massive lens, a NFW distribution with $M_{200} \simeq 10^{15}\,{\rm M}_\odot$ and $c_{200} \simeq 3$. The deviation of the slope from the isothermal value is small over a large radial range, with $\delta\gamma(r_{2500}) \simeq 0.4$, $\delta\gamma(r_{500}) \simeq 0.0$, $\delta\gamma(r_{200}) \simeq -0.1$ and $\delta\gamma(r_{\rm vir}) \simeq -0.2$.

To make the proper conversion from different cosmological parameters, I used by default $\delta\gamma = 0$, when equation (21) reduces to

$$M_\Delta^{\rm WL} \propto \left(\frac{D_{\rm ds}}{D_{\rm s}}\right)^{-3/2} H(z)^{-1}. \quad (23)$$

Equation (22) can be simplified as

$$M_{\rm vir}^{\rm WL} \propto \Delta_{\rm vir}(\Omega_{\rm M})^{-\frac{1}{2}} \left(\frac{D_{\rm ds}}{D_{\rm s}}\right)^{-3/2} H(z)^{-1}. \quad (24)$$

6 CATALOGUE COMPILATION

I included in the catalogue all groups and clusters with WL analyses I was aware of. The search of the literature was performed thanks to NASA's Astrophysics Data System.[3] A public list of clusters with WL analyses, compiled by H. Dahle and last updated in 2007, was also used.[4]

The compilation of the first versions of the catalogues was based on 69 WL studies comprising 822 analyses of individual groups and clusters; see Table 1.

[3] http://www.adsabs.harvard.edu/
[4] http://folk.uio.no/hdahle/WLclusters.html

The catalogues aimed to avoid re-elaboration as much as possible. Masses quoted in the reference papers were directly reported. When original estimates were provided with asymmetric errors, I computed the mean value and the standard deviation as suggested in D'Agostini (2004). Missing masses were computed by

Table 1. Number of clusters, groups or substructures ($N_{\rm clusters}$ in column 3), analysed in each reference, column 1. The authors' code is listed in column 2.

Reference	Code	$N_{\rm clusters}$
Shan et al. (2012)	shan+12	87
Hoekstra et al. (2012)	hoekstra+12	55
Applegate et al. (2014)	applegate+14	51
Mahdavi et al. (2013)	mahdavi+13	50
Dahle et al. (2002)	dahle+02	38
McInnes et al. (2009)	mcinnes+09	36
Dahle (2006)	dahle06	35
Sereno & Covone (2013)	sereno&13	31
Okabe et al. (2010)	okabe+10	30
Pedersen & Dahle (2007)	pedersen&07	30
Oguri et al. (2012)	oguri+12	28
Hamana et al. (2009)	hamana+09	27
Jee et al. (2011)	jee+11	27
Hoekstra et al. (2011)	hoekstra+11	25
Cypriano et al. (2004)	cypriano+04	24
Clowe et al. (2006)	clowe+06	20
Umetsu et al. (2014)	umetsu+14	20
Merten et al. (2014)	merten+14	19
Gruen et al. (2014)	gruen+14	12
Limousin et al. (2009)	limousin+09	12
Bardeau et al. (2007)	bardeau+07	11
Foëx et al. (2012)	foex+12	11
Kettula et al. (2013)	kettula+13	10
Smail et al. (1997)	smail+97	10
Abate et al. (2009)	abate+09	9
Okabe & Umetsu (2008)	okabe&08	9
Gavazzi & Soucail (2007)	gavazzi&07	8
Israel et al. (2012)	israel+12	8
Kubo et al. (2009)	kubo+09	7
Watanabe et al. (2011)	watanabe+11	6
Clowe et al. (2000)	clowe+00	6
High et al. (2012)	high+12	5
Umetsu et al. (2011)	umetsu+11	5
Okabe et al. (2011)	okabe+11	4
Umetsu et al. (2009)	umetsu+09	4
Melchior et al. (2014)	melchior+14	4
Okabe et al. (2014b)	okabe+14b	4
Corless et al. (2009)	corless+09	3
Gray et al. (2002)	grey+02	3
Gavazzi et al. (2004)	gavazzi+04	3
Jee et al. (2014)	jee+14	3
Bradač et al. (2006)	bradac+06	2
Hamilton-Morris et al. (2012)	Hamilton-morris+12	2
Dietrich et al. (2009)	dietrich+09	2
Bradač et al. (2008a)	bradac+08b	2
Bradač et al. (2008b)	bradac+08a	1
Clowe, Gonzalez & Markevitch (2004)	clowe+04	1
Gavazzi (2005)	gavazzi05	1
Gavazzi et al. (2009)	gavazzi+09	1
Halkola, Seitz & Pannella (2006)	halkola+06	1
Hicks et al. (2007)	hicks+07	1
Huang et al. (2011)	huang+11	1
Jauzac et al. (2012)	jauzac+12	1
Jauzac et al. (2014)	jauzac+14	1
Kubo et al. (2007)	kubo+07	1

Table 1. – *continued*

Reference	Code	$N_{\rm clusters}$
Lerchster et al. (2011)	lerchster+11	1
Limousin et al. (2007)	limousin+07	1
Limousin et al. (2010)	limousin+10	1
Mahdavi et al. (2007)	mahdavi+07	1
Margoniner et al. (2005)	margoniner+05	1
Merten et al. (2011)	merten+11	1
Miyatake et al. (2013)	miyatake+13	1
Oguri et al. (2013)	oguri+13	1
Okabe et al. (2014a)	okabe+14a	1
Paulin-Henriksson et al. (2007)	paulin-henriksson+07	1
Radovich et al. (2008)	radovich+08	1
Romano et al. (2010)	romano+10	1
Schirmer et al. (2010)	schirmer+10	1
Schirmer et al. (2011)	schirmer+11	1

extrapolation as discussed in Section 4. Corrections for the cosmological model were performed as detailed in Section 5.

Masses were redetermined in three cases with the fit procedure detailed in Sereno et al. (2015). Briefly, the observed shear profile is fitted to a spherical NFW functional through the function,

$$\chi^2_{\rm WL}(M_{200}, c_{200}) = \sum_i \left[\frac{g_+(\theta_i) - g_+^{\rm NFW}(\theta_i; M_{200}, c_{200})}{\delta_+(\theta_i)} \right]^2, \quad (25)$$

where g_+ is the reduced tangential shear at angular position θ and δ_+ is the observational uncertainty.

When a strong lensing constraint was available, the effective angular Einstein radius $\theta_{\rm E}$ was fitted through

$$\chi^2_{\rm SL}(M_{200}, c_{200}) = \left[\frac{\theta_{\rm E} - \theta_{\rm E}^{\rm NFW}(M_{200}, c_{200})}{\delta\theta_{\rm E}} \right]^2. \quad (26)$$

Expressions for the lensing quantities of the NFW halo can be found in Bartelmann (1996) and Wright & Brainerd (2000). The total likelihood is $\mathcal{L} \propto \exp\{-(\chi^2_{\rm WL} + \chi^2_{\rm SL})/2\}$. For the catalogue, I considered uniform priors in the ranges $0.02 \leq M_{200}/(10^{14} h^{-1}\,{\rm M}_\odot) \leq 100$ and $0.02 \leq c_{200} \leq 20$. The parameters and their uncertainties were finally derived as the bi-weight estimators of the marginalised posterior probability densities.

For the Local Cluster Substructure Survey (LOCUSS) sample in Okabe et al. (2010), I fitted the published shear profiles to derive the masses of all the 30 clusters of the sample, rather than the 26 reported in Okabe et al. (2010, table 6). Shear measurements in Okabe et al. (2010) are biased low due to contamination effects and systematics in shape measurements (Okabe et al. 2013). We then corrected the fitted masses according to the factors reported in Okabe et al. (2013, table 2).

I also refitted the clusters previously analysed in Sereno & Covone (2013). The fit procedure has been slightly improved since; see Sereno et al. (2015). For the catalogue, I used the updated mass determinations.

Finally, Mahdavi et al. (2007) published the shear profile of ABELL 478 but they did not report the mass determination. Values listed in the catalogues are the result of the fit procedure I performed.

6.1 Intentional omissions

There were a number of intentional omissions. I required that each lensing cluster was confirmed by independent observations. Lensing peaks without an optical, X-ray or SZ counterpart were excised from the catalogue. This may be the case for some WL shear-selected haloes or lensing peaks found in pilot programmes targeting fields centred on active galactic nuclei or quasars (Wold et al. 2002).

I did not include some lensing analyses of single clusters that were later refined or improved by the same authors or collaboration. As an example, this is the case for the analyses of the high redshift clusters in Jee et al. (2005a, 2005b), Jee et al. (2006) and Jee & Tyson (2009), which were later revised in Jee et al. (2011).

I considered only lensing studies performed under the assumption of spherical symmetry. Unfortunately, there is just a handful of clusters with triaxial analyses (Oguri et al. 2005; Corless et al. 2009; Sereno & Umetsu 2011; Sereno et al. 2013; Morandi et al. 2012; Limousin et al. 2013, and references therein). For homogeneity reasons, I excluded them.

Complex cluster morphologies may be separated in multiple peaks by high resolution WL analyses. To compile the catalogue with unique entries, LC^2-*single*, I only considered masses measured with a single halo analysis. Masses of substructures and multiple peaks associated with the same clusters are reported in LC^2-*substructure*.

6.2 Cluster identification

The same cluster may appear in several analyses under different names and with different quoted redshifts and locations. To standardize the notation, I reported the NASA/IPAC Extragalactic Database[5] (NED) preferred name and NED's coordinates and redshift for each object. Most of the clusters were identified by name. A few of them were associated by matching positions.

Since most of the lenses that are not associated by name in NED are secondary haloes in merging or complex systems, or shear-selected peaks found in dense fields, I could not adopt a fixed search radius when cross-checking with NED. In fact, a blind matching based on a fixed aperture can associate the same NED counterpart with multiple, separate lenses, which we know to be distinct according to the reference paper. The association by position was then performed cluster by cluster. A limited number of lenses, mostly SZ or shear-selected haloes, lacked an NED identification.

Control of repeated entries was performed by looking for repeated NED associations. For clusters that were not identified by querying NED, I also looked for matches of both position and redshift. If the cluster's coordinates were missing in the original papers, I used the location obtained from querying NED.

7 CATALOGUE PRESENTATION

I compiled three catalogues. LC^2-*single* lists all clusters and groups whose mass was determined by single-halo modelling, no matter what the dynamical state, and contains virtually no multiple entries.

LC^2-*substructure* lists separately the main components and the secondary haloes of complex systems whose masses were derived with a multiple-halo analysis. As for LC^2-*single*, duplicate entries were eliminated. There is some redundancy between LC^2-*single* and LC^2-*substructure*. Some systems may appear as a single halo in LC^2-*single* and as a main halo with substructures in LC^2-*substructure*.

LC^2-*all* comprises the full body of information I found and reduced from the literature. Multiple entries are present, as well as single- or multiple-halo analyses of the same lens. LC^2-*single* and

[5] http://ned.ipac.caltech.edu/

Table 2. The first 50 entries of the LC^2-single catalogue. The full catalogues are available in electronic form. Columns are described in Section 8.

Name	RA (J2000)	Declination (J2000)	z	Match	NED's primary name	NED's RA (J2000)	NED's DEC (J2000)	NED's z	Author code	ADS's bibcode	M_{2500} [10^{14} M$_\odot$]	δM_{2500} [10^{14} M$_\odot$]	M_{500} [10^{14} M$_\odot$]	δM_{500} [10^{14} M$_\odot$]	M_{200} [10^{14} M$_\odot$]	δM_{200} [10^{14} M$_\odot$]	$M_{\rm vir}$ [10^{14} M$_\odot$]	$\delta M_{\rm vir}$ [10^{14} M$_\odot$]
(1–2)	(3)	(4)	(5)	(6)	(7-8)	(9)	(10)	(11)	(12)	(13)	(14)	(15)	(16)	(17)	(18)	(19)	(20)	(21)
ABELL 2744	00:14:20.67	−30:24:00.86	0.308	N	ABELL 2744	00:14:18.90	−30:23:22.0	0.308	merten+11	2011MNRAS.417..333M	4.962	1.597	15.412	4.959	24.054	7.741	29.025	9.340
CL 0016+16	00:18:33.445	+16:26:13.00	0.547	N	Cl 0016+16	00:18:33.84	+16:26:16.6	0.541	applegate+14	2014MNRAS.439...48A	7.122	1.842	17.821	4.609	25.756	6.661	29.101	7.526
ABELL 22	00:20:38.6	−25:43:19.2	0.141	N	ABELL 22	00:20:42.80	−25:42:37.0	0.142352	cypriano+04	2004ApJ...613...95C	1.012	0.512	2.263	1.146	3.578	1.812	4.760	2.410
ACT-CL J0022.2-0036	00:22:13.0	−00:36:33.8	0.805	NA	NA NA	NA	NA	NA	miyatake+13	2013MNRAS.429.3627M	2.824	1.456	7.860	4.053	11.798	6.083	13.118	6.764
MACS J0025.4-1222	00:25:29.907	−12:22:44.64	0.585	N	MACS J0025.4-1222	00:25:29.38	−12:22:37.1	0.5843	applegate+14	2014MNRAS.439...48A	3.965	1.392	9.922	3.483	14.340	5.034	16.130	5.663
Cl 0024+17	00:26:36.0	+17:08:36	0.39	N	ZwCl 0024.0+1652	00:26:35.70	+17:09:46.0	0.39	umetsu+11	2011ApJ...729..127U	6.600	0.900	12.329	1.943	17.057	2.686	18.986	3.200
CL 0030+2618	00:30:33.6	+26:18:16	0.5	N	WARP J0030.5+2618	00:30:33.20	+26:18:19.0	0.5	israel+12	2012A%26A...546A..79I	1.803	0.516	4.512	1.292	6.521	1.867	7.412	2.122
ABELL 68	00:37:05.947	+09:09:36.02	0.255	N	ABELL 68	00:37:05.30	+09:09:11.0	0.255	applegate+14	2014MNRAS.439...48A	3.665	0.634	9.171	1.587	13.254	2.294	15.670	2.712
ABELL 85	00:41:48.7	−09:19:04.8	0.056	N	ABELL 85	00:41:50.10	−09:18:07.0	0.055061	cypriano+04	2004ApJ...613...95C	2.048	0.557	4.579	1.245	7.240	1.968	9.947	2.704
ABELL 2811	00:42:07.9	−28:32:09.6	0.108	N	ABELL 2811	00:42:08.70	−28:32:09.0	0.107908	cypriano+04	2004ApJ...613...95C	1.767	0.849	3.952	1.898	6.248	3.000	8.414	4.040
ABELL 115	00:55:59.8	+26:22:40.8	0.1971	N	ABELL 115	00:55:59.80	+26:22:41.0	0.1971	okabe+10	2010PASJ...62..811O	1.478	0.936	4.832	3.061	7.427	4.705	9.108	5.771
Cl 0054-27	00:56:37.4	−27:30:47	0.56	N	ABELL 2843	00:56:37.38	−27:30:46.7	0.56	smail+97	1997ApJ...479...70S	1.131	0.619	3.391	1.857	5.227	2.862	6.012	3.292
RX J0056.9-2740	00:56:56.98	−27:40:29.9	0.563	N	Cl 0054-2756	00:56:56.87	−27:40:30.1	0.56	hoekstra+11	2011ApJ...726...48H	0.640	0.360	1.862	1.048	2.840	1.597	3.255	1.831
ACT-CL J0102-4915	01:02:52.50	−49:14:58.0	0.87	N	SPT-CL J0102-4915	01:02:53.00	−49:15:19.0	0.75	jee+14	2014ApJ...785...20J	4.391	0.847	16.800	3.200	25.400	4.900	28.661	5.529
ABELL 141	01:05:36.3	−24:39:20	0.23	N	ABELL 141	01:05:34.80	−24:39:17.0	0.23	dahle+02	2002ApJS..139..313D	3.225	1.301	7.212	2.909	11.403	4.599	14.723	5.939
ZwCl 0104.4+0048	01:06:48.5	+01:02:42.0	0.2545	N	ZwCl 0104.4+0048	01:06:58.07	+01:04:01.4	0.2545	okabe+10	2010PASJ...62..811O	1.008	0.262	1.841	0.478	2.299	0.597	2.546	0.661
RX J0110.3+1938	01:10:18.22	+19:38:19.4	0.317	N	WARP J0110.3+1938	01:10:18.00	+19:38:23.0	0.317	hoekstra+11	2011ApJ...726...48H	0.580	0.300	1.585	0.820	2.363	1.222	2.796	1.446
ABELL 209	01:31:52.54	−13:36:40.4	0.206	N	ABELL 209	01:31:53.00	−13:36:34.0	0.206	umetsu+14	2014arXiv1404.1375U	4.033	0.688	11.573	1.796	17.559	2.993	21.473	3.922
ABELL 222	01:37:34.0	−12:59:29	0.213	N	ABELL 222	01:37:29.20	−12:59:10.0	0.213	mahdavi+13	2013ApJ...767..116M	1.572	0.555	5.649	1.246	8.559	1.888	10.417	2.298
ABELL 223S	01:37:56.0	−12:49:10	0.207	NA	NA NA	NA	NA	NA	mahdavi+13	2013ApJ...767..116M	1.003	0.482	6.863	1.936	10.435	2.943	12.738	3.593
ABELL 223N	01:38:02.3	−12:45:20	0.207	NA	NA NA	NA	NA	NA	hoekstra+12	2012MNRAS.427.1298H	2.100	0.550	5.500	1.900	8.320	2.142	10.100	2.600
RX J0142.0+2131	01:42:03.311	+21:31:22.64	0.28	N	MCXC J0142.0+2131	01:42:02.60	+21:31:19.0	0.2803	applegate+14	2014MNRAS.439...48A	1.847	0.743	4.621	1.860	6.678	2.688	7.858	3.162
CL J0152-1357	01:52:41.0	−13:57:45	0.84	N	WARP J0152.7-1357	01:52:41.00	−13:57:45.0	0.831	sereno&13	2013MNRAS.434..878S	1.382	0.291	2.259	0.475	2.800	0.589	2.964	0.624
ABELL 267	01:52:42.0	+01:00:26	0.23	N	ABELL 267	01:52:52.26	+01:02:45.8	0.231	mahdavi+13	2013ApJ...767..116M	2.053	0.428	5.245	1.523	7.948	2.308	9.637	2.798
RX J0154.2-5937	01:54:13.72	−59:37:31.0	0.36	N	400d J0154-5937	01:54:14.80	−59:37:48.0	0.36	hoekstra+11	2011ApJ...726...48H	0.340	0.200	0.910	0.535	1.348	0.793	1.578	0.928
CL 0159+0030	01:59:18.2	+00:30:09	0.39	N	NSCS J015924+003024	01:59:17.00	+00:30:10.4	0.386	israel+12	2012A%26A...546A..79I	1.443	0.634	3.466	1.524	4.937	2.170	5.671	2.493
CFHTLS c12-w1	02:01:18.00	−07:39:03.60	0.14	NA	NA NA	NA	NA	NA	shan+12	2012ApJ...748...56S	0.107	0.023	0.259	0.055	0.371	0.078	0.447	0.095
CFHTLS c3-w1	02:01:41.04	−05:01:48.00	0.28	NA	NA NA	NA	NA	NA	shan+12	2012ApJ...748...56S	0.987	0.183	2.813	0.522	4.257	0.790	5.104	0.947
ABELL 291	02:01:44.2	−02:12:03.0	0.196	N	ABELL 291	02:01:44.20	−02:12:03.0	0.197	okabe+10	2010PASJ...62..811O	1.166	0.345	5.222	1.545	9.022	2.669	11.658	3.448
CFHTLS c16-w1	02:01:48.48	−10:51:10.80	0.66	NA	NA NA	NA	NA	NA	shan+12	2012ApJ...748...56S	0.617	0.094	1.870	0.284	2.892	0.440	3.289	0.500
CFHTLS c14-w1	02:02:08.16	−08:26:13.20	0.4	P	GMBCG J030.53418-08.43703	02:02:08.20	−08:26:13.3	0.349	shan+12	2012ApJ...748...56S	0.458	0.054	1.285	0.151	1.934	0.227	2.262	0.266
CFHTLS c2-w1	02:02:30.00	−03:57:57.60	0.48	NA	NA NA	NA	NA	NA	shan+12	2012ApJ...748...56S	4.884	2.826	16.261	9.408	26.022	15.057	30.663	17.742
CFHTLS c13-w1	02:02:49.92	−09:20:13.20	0.23	P	ABELL 298	02:02:48.90	−09:19:57.0	0.14315	shan+12	2012ApJ...748...56S	0.054	0.031	0.130	0.075	0.185	0.107	0.219	0.126
CFHTLS c6-w1	02:03:21.60	−07:19:51.60	0.27	NA	NA NA	NA	NA	NA	shan+12	2012ApJ...748...56S	0.258	0.057	0.678	0.150	0.997	0.221	1.184	0.262
CFHTLS c5-w1	02:03:26.40	−05:55:30.00	0.38	NA	NA NA	NA	NA	NA	shan+12	2012ApJ...748...56S	0.246	0.052	0.662	0.139	0.981	0.206	1.146	0.241
CFHTLS c15-w1	02:03:28.80	−09:49:01.20	0.32	P	GMBCG J030.86962-09.81667	02:03:28.71	−09:49:00.0	0.33	shan+12	2012ApJ...748...56S	0.220	0.055	0.580	0.145	0.854	0.213	1.005	0.251
CFHTLS c9-w1	02:03:32.16	−06:44:09.60	0.81	NA	NA NA	NA	NA	NA	shan+12	2012ApJ...748...56S	1.042	0.261	3.371	0.845	5.339	1.338	6.012	1.507
CFHTLS c1-w1	02:03:57.60	−04:13:22.80	0.18	NA	NA NA	NA	NA	NA	shan+12	2012ApJ...748...56S	1.956	1.176	5.652	3.398	8.597	5.168	10.562	6.350
CFHTLS c7-w1	02:04:18.48	−07:12:46.80	0.33	NA	NA NA	NA	NA	NA	shan+12	2012ApJ...748...56S	0.682	0.486	1.924	1.372	2.903	2.070	3.442	2.455
CFHTLS c22-w1	02:05:05.28	−05:55:22.80	0.41	NA	NA NA	NA	NA	NA	shan+12	2012ApJ...748...56S	0.088	0.055	0.224	0.141	0.327	0.206	0.377	0.238
CFHTLS c26-w1	02:05:16.80	−07:40:48.00	0.24	NA	NA NA	NA	NA	NA	shan+12	2012ApJ...748...56S	0.169	0.056	0.431	0.142	0.627	0.207	0.745	0.246
CFHTLS c24-w1	02:05:25.92	−07:35:16.80	0.4	P	CFHTLS:[DAC2011] W1-0493	02:05:25.92	−07:35:22.6	0.47	shan+12	2012ApJ...748...56S	0.455	0.185	1.275	0.520	1.919	0.782	2.245	0.915
CFHTLS c27-w1	02:06:22.80	−08:48:25.20	0.26	NA	NA NA	NA	NA	NA	shan+12	2012ApJ...748...56S	0.653	0.414	1.807	1.146	2.706	1.716	3.244	2.057
CFHTLS c28-w1	02:07:04.56	−08:29:42.00	0.08	NA	NA NA	NA	NA	NA	shan+12	2012ApJ...748...56S	0.230	0.066	0.574	0.163	0.828	0.236	1.016	0.289
CFHTLS c18-w1	02:07:11.28	−04:00:07.20	0.25	NA	NA NA	NA	NA	NA	shan+12	2012ApJ...748...56S	2.256	1.374	6.711	4.087	10.313	6.282	12.523	7.628
CFHTLS c17-w1	02:08:05.04	−04:34:58.80	0.32	NA	NA NA	NA	NA	NA	shan+12	2012ApJ...748...56S	2.035	1.135	6.130	3.420	9.464	5.280	11.343	6.328
CFHTLS c39-w1	02:08:32.40	−07:43:48.00	0.34	NA	NA NA	NA	NA	NA	shan+12	2012ApJ...748...56S	0.817	0.528	2.337	1.511	3.543	2.291	4.200	2.716
CFHTLS c42-w1	02:09:15.12	−09:14:38.40	0.71	NA	NA NA	NA	NA	NA	shan+12	2012ApJ...748...56S	0.382	0.148	1.135	0.438	1.743	0.673	1.967	0.760
CFHTLS c33-w1	02:09:44.40	−05:43:48.00	0.23	NA	NA NA	NA	NA	NA	shan+12	2012ApJ...748...56S	0.340	0.038	0.899	0.101	1.325	0.150	1.588	0.179
ABELL 315	02:10:03.0	−00:59:52	0.1754	N	ABELL 315	02:10:03.06	−00:59:51.8	0.1754	dietrich+09	2009A%26A...499..669D	1.172	0.331	3.215	0.909	4.800	1.357	5.854	1.655

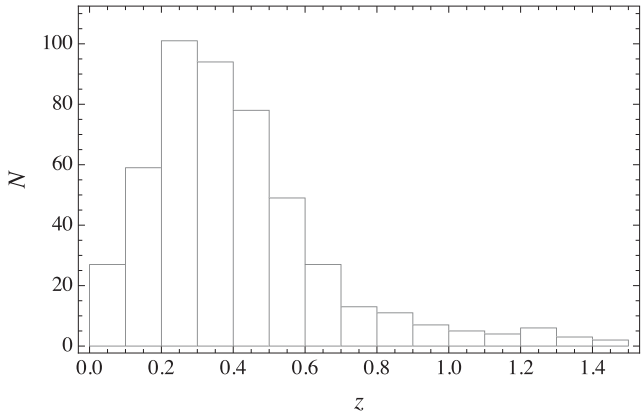

Figure 2. Redshift distribution of the 485 WL clusters in the LC^2-*single* catalogue.

LC^2-*substructure* are subsamples with unique entries from LC^2-*all*. When a cluster had multiple analyses in the literature, I picked for LC^2-*single* either the most recent analysis or that based on deeper observations.

Table 2 presents an extract of the first 50 entries of LC^2-*single*. In each catalogue, objects are ordered by right ascension. The format is as follows:

Columns 1 and 2: Name of cluster as designated in the original lensing paper.

Columns 3 and 4: Right ascension (RA) (J2000) and declination (DEC) (J2000), as quoted in the original lensing paper. If coordinates are not quoted in the source paper or in a companion one, I reported the coordinates for the NED association.

Column 5: Redshift z, as reported in the original lensing paper.

Column 6: External validation through NED. N: the NED object was associated by name; P: the NED object was associated by positional matching; NA: no association found.

Columns 7–11: As in columns 1–5, but for the NED association.

Column 12: Author code.

Column 13: ADS bibliographic code.

Columns 14 and 15: Over-density mass M_{2500} and related uncertainty δM_{2500}, in units of 10^{14} M$_\odot$.

Columns 16 and 17: As for columns 14 and 15, but for the over-density mass M_{500}.

Columns 18 and 19: As for columns 14 and 15, but for the over-density mass M_{200}.

Columns 20 and 21: As for columns 14 and 15, but for the virial mass $M_{\rm vir}$.

7.1 Basic properties

Here, I discuss the basic properties of the collected clusters: 507 clusters, groups or substructures were analysed in published lensing studies and 131 objects were studied by at least two independent groups. The most popular targets are ABELL 209, 1835 and 2261, with 10 independent analyses each, and ABELL 611 and 1689 (nine analyses each). Overall, we found 822 mass determinations.

The *single* catalogue contains 485 unique entries. The redshift distribution of the (unique) clusters (see Fig. 2) has a large range, $0.02 \lesssim z \lesssim 1.46$, with a peak at $z \sim 0.35$, where lensing studies are optimized. The tail at large redshift includes 50 (20) clusters at $z >$ 0.7 (1.0).

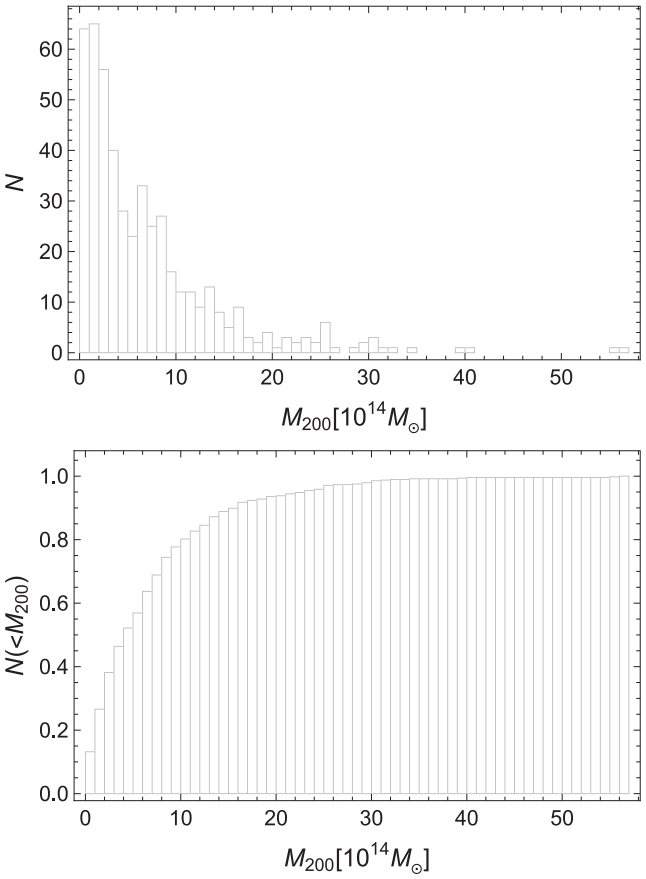

Figure 3. Mass distribution of the 485 WL clusters in the LC^2-*single* catalogue. Top panel: Histogram of the mass distribution. Bottom panel: Normalized cumulative function. M_{200} is in units of 10^{14} M$_\odot$.

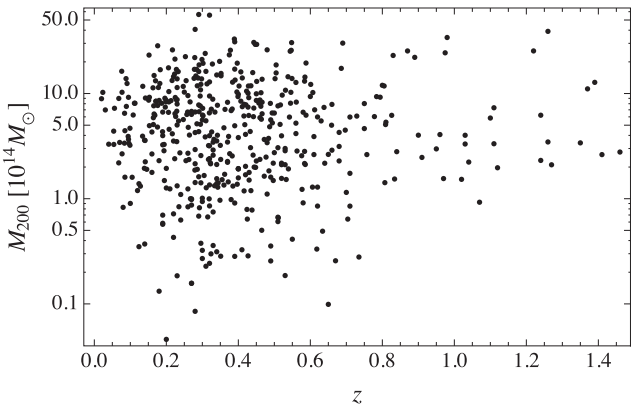

Figure 4. Redshift versus mass for the 485 WL clusters in the LC^2-*single* catalogue. M_{200} is in units of 10^{14} M$_\odot$.

WL is better suited to measure massive clusters. The mass distribution has a median $M_{200} \sim 4.5 \times 10^{14}$ M$_\odot$ and extends to M_{200} larger than 5×10^{15} M$_\odot$; see Fig. 3. Shear or X-ray selected groups of clusters mostly populate the less massive bins.

Due to the heterogeneous nature of the sample, there is no evident trend in cluster masses with redshift; see Fig. 4. Approximate selection functions can be derived only for specific subsamples.

8 CONCLUSIONS

A standardized collection of WL masses can be useful for X-ray, SZ and other multi-wavelength studies. I compiled from the literature three catalogues. The LC^2-*all*, -*single* and -*substructure* catalogues comprise 822, 485 and 18 groups and clusters, respectively.

The LC^2-*all* catalogue is a repository of all the main information on clusters with measured lensing mass I found in the literature. LC^2-*single* is a list of unique entries. LC^2-*substructure* focuses on complex structures.

The full catalogues are publicly available in electronic format.[6] The first version of the catalogues is released together with this presentation paper too. The catalogues will be periodically updated.

ACKNOWLEDGEMENTS

I thank S. Ettori, L. Moscardini and K. Umetsu for fruitful discussions. I acknowledge financial contributions from contracts ASI/INAF n.I/023/12/0 'Attività relative alla fase B2/C per la missione Euclid', PRIN MIUR 2010-2011 'The dark Universe and the cosmic evolution of baryons: from current surveys to Euclid', and PRIN INAF 2012 'The Universe in the box: multiscale simulations of cosmic structure'. I thank NASA. This research has made use of NASA's Astrophysics Data System (ADS) and the NASA/IPAC Extragalactic Database (NED), which is operated by the Jet Propulsion Laboratory, California Institute of Technology, under contract with the National Aeronautics and Space Administration.

REFERENCES

Abate A., Wittman D., Margoniner V. E., Bridle S. L., Gee P., Tyson J. A., Dell'Antonio I. P., 2009, ApJ, 702, 603
Andreon S., Bergé J., 2012, A&A, 547, A117
Applegate D. E. et al., 2014, MNRAS, 439, 48
Arnaud M., Pratt G. W., Piffaretti R., Böhringer H., Croston J. H., Pointecouteau E., 2010, A&A, 517, A92
Bahé Y. M., McCarthy I. G., King L. J., 2012, MNRAS, 421, 1073
Bardeau S., Soucail G., Kneib J.-P., Czoske O., Ebeling H., Hudelot P., Smail I., Smith G. P., 2007, A&A, 470, 449
Bartelmann M., 1996, A&A, 313, 697
Bartelmann M., Schneider P., 2001, Phys. Rep., 340, 291
Becker M. R., Kravtsov A. V., 2011, ApJ, 740, 25
Bhattacharya S., Habib S., Heitmann K., Vikhlinin A., 2013, ApJ, 766, 32
Biviano A. et al., 2013, A&A, 558, A1
Bradač M. et al., 2006, ApJ, 652, 937
Bradač M., Allen S. W., Treu T., Ebeling H., Massey R., Morris R. G., von der Linden A., Applegate D., 2008a, ApJ, 687, 959
Bradač M. et al., 2008b, ApJ, 681, 187
Bryan G. L., Norman M. L., 1998, ApJ, 495, 80
Clowe D., Luppino G. A., Kaiser N., Gioia I. M., 2000, ApJ, 539, 540
Clowe D., Gonzalez A., Markevitch M., 2004, ApJ, 604, 596
Clowe D. et al., 2006, A&A, 451, 395
Corless V. L., King L. J., Clowe D., 2009, MNRAS, 393, 1235
Cypriano E. S., Sodré L., Jr, Kneib J.-P., Campusano L. E., 2004, ApJ, 613, 95
D'Agostini G., 2004, physics/0403086
Dahle H., 2006, ApJ, 653, 954
Dahle H., Kaiser N., Irgens R. J., Lilje P. B., Maddox S. J., 2002, ApJS, 139, 313
Diemer B., Kravtsov A. V., 2015, ApJ, 799, 108
Dietrich J. P., Biviano A., Popesso P., Zhang Y.-Y., Lombardi M., Böhringer H., 2009, A&A, 499, 669
Donahue M. et al., 2014, ApJ, 794, 136
Duffy A. R., Schaye J., Kay S. T., Dalla Vecchia C., 2008, MNRAS, 390, L64
Dutton A. A., Macciò A. V., 2014, MNRAS, 441, 3359
Ettori S., 2013, MNRAS, 435, 1265
Ettori S., Morandi A., Tozzi P., Balestra I., Borgani S., Rosati P., Lovisari L., Terenziani F., 2009, A&A, 501, 61
Foëx G., Soucail G., Pointecouteau E., Arnaud M., Limousin M., Pratt G. W., 2012, A&A, 546, A106
Gao L., Navarro J. F., Cole S., Frenk C. S., White S. D. M., Springel V., Jenkins A., Neto A. F., 2008, MNRAS, 387, 536
Gavazzi R., 2005, A&A, 443, 793
Gavazzi R., Soucail G., 2007, A&A, 462, 459
Gavazzi R., Mellier Y., Fort B., Cuillandre J.-C., Dantel-Fort M., 2004, A&A, 422, 407
Gavazzi R., Adami C., Durret F., Cuillandre J.-C., Ilbert O., Mazure A., Pelló R., Ulmer M. P., 2009, A&A, 498, L33
Giocoli C., Meneghetti M., Ettori S., Moscardini L., 2012, MNRAS, 426, 1558
Giocoli C., Meneghetti M., Metcalf R. B., Ettori S., Moscardini L., 2014, MNRAS, 440, 1899
Giodini S., Lovisari L., Pointecouteau E., Ettori S., Reiprich T. H., Hoekstra H., 2013, Space Sci. Rev., 177, 247
Gott J. R., III, Vogeley M. S., Podariu S., Ratra B., 2001, ApJ, 549, 1
Gray M. E., Taylor A. N., Meisenheimer K., Dye S., Wolf C., Thommes E., 2002, ApJ, 568, 141
Gruen D. et al., 2014, MNRAS, 442, 1507
Halkola A., Seitz S., Pannella M., 2006, MNRAS, 372, 1425
Hamana T., Miyazaki S., Kashikawa N., Ellis R. S., Massey R. J., Refregier A., Taylor J. E., 2009, PASJ, 61, 833
Hamilton-Morris V., Smith G. P., Edge A. C., Egami E., Haines C. P., Marshall P. J., Sanderson A. J. R., Targett T. A., 2012, ApJ, 748, L23
Hicks A. K. et al., 2007, ApJ, 671, 1446
High F. W. et al., 2012, ApJ, 758, 68
Hoekstra H., Donahue M., Conselice C. J., McNamara B. R., Voit G. M., 2011, ApJ, 726, 48
Hoekstra H., Mahdavi A., Babul A., Bildfell C., 2012, MNRAS, 427, 1298
Hu W., Kravtsov A. V., 2003, ApJ, 584, 702
Huang Z., Radovich M., Grado A., Puddu E., Romano A., Limatola L., Fu L., 2011, A&A, 529, A93
Israel H., Erben T., Reiprich T. H., Vikhlinin A., Sarazin C. L., Schneider P., 2012, A&A, 546, A79
Jauzac M. et al., 2012, MNRAS, 426, 3369
Jauzac M. et al., 2014, preprint (arXiv:1406.3011)
Jee M. J., Tyson J. A., 2009, ApJ, 691, 1337
Jee M. J., White R. L., Benítez N., Ford H. C., Blakeslee J. P., Rosati P., Demarco R., Illingworth G. D., 2005a, ApJ, 618, 46
Jee M. J., White R. L., Ford H. C., Blakeslee J. P., Illingworth G. D., Coe D. A., Tran K.-V. H., 2005b, ApJ, 634, 813
Jee M. J., White R. L., Ford H. C., Illingworth G. D., Blakeslee J. P., Holden B., Mei S., 2006, ApJ, 642, 720
Jee M. J. et al., 2011, ApJ, 737, 59
Jee M. J., Hughes J. P., Menanteau F., Sifón C., Mandelbaum R., Barrientos L. F., Infante L., Ng K. Y., 2014, ApJ, 785, 20
Jing Y. P., Suto Y., 2002, ApJ, 574, 538
Jullo E., Natarajan P., Kneib J.-P., D'Aloisio A., Limousin M., Richard J., Schimd C., 2010, Science, 329, 924
Kettula K. et al., 2013, ApJ, 778, 74
Kubo J. M., Stebbins A., Annis J., Dell'Antonio I. P., Lin H., Khiabanian H., Frieman J. A., 2007, ApJ, 671, 1466
Kubo J. M. et al., 2009, ApJ, 702, L110
LaRoque S. J., Bonamente M., Carlstrom J. E., Joy M. K., Nagai D., Reese E. D., Dawson K. S., 2006, ApJ, 652, 917
Laureijs R. et al., 2011, preprint (arXiv:1110.3193)
Lemze D., Broadhurst T., Rephaeli Y., Barkana R., Umetsu K., 2009, ApJ, 701, 1336
Lerchster M. et al., 2011, MNRAS, 411, 2667
Limousin M. et al., 2007, ApJ, 668, 643

[6] http://pico.bo.astro.it/~sereno/CoMaLit/LC2/

Limousin M. et al., 2009, A&A, 502, 445
Limousin M. et al., 2010, MNRAS, 405, 777
Limousin M., Morandi A., Sereno M., Meneghetti M., Ettori S., Bartelmann M., Verdugo T., 2013, Space Sci. Rev., 177, 155
Lubini M., Sereno M., Coles J., Jetzer P., Saha P., 2014, MNRAS, 437, 2461
Mahdavi A., Hoekstra H., Babul A., Sievers J., Myers S. T., Henry J. P., 2007, ApJ, 664, 162
Mahdavi A., Hoekstra H., Babul A., Bildfell C., Jeltema T., Henry J. P., 2013, ApJ, 767, 116
Mantz A., Allen S. W., Rapetti D., Ebeling H., 2010, MNRAS, 406, 1759
Margoniner V. E., Lubin L. M., Wittman D. M., Squires G. K., 2005, AJ, 129, 20
McInnes R. N., Menanteau F., Heavens A. F., Hughes J. P., Jimenez R., Massey R., Simon P., Taylor A., 2009, MNRAS, 399, L84
Medezinski E., Broadhurst T., Umetsu K., Oguri M., Rephaeli Y., Benítez N., 2010, MNRAS, 405, 257
Melchior P. et al., 2014, preprint (arXiv:1405.4285)
Menanteau F. et al., 2013, ApJ, 765, 67
Meneghetti M., Rasia E., Merten J., Bellagamba F., Ettori S., Mazzotta P., Dolag K., Marri S., 2010, A&A, 514, A93
Meneghetti M., Fedeli C., Zitrin A., Bartelmann M., Broadhurst T., Gottlöber S., Moscardini L., Yepes G., 2011, A&A, 530, A17
Merten J. et al., 2011, MNRAS, 417, 333
Merten J. et al., 2014, preprint (arXiv:1404.1376)
Miyatake H. et al., 2013, MNRAS, 429, 3627
Morandi A. et al., 2012, MNRAS, 425, 2069
Navarro J. F., Frenk C. S., White S. D. M., 1996, ApJ, 462, 563
Neto A. F. et al., 2007, MNRAS, 381, 1450
Oguri M., Blandford R. D., 2009, MNRAS, 392, 930
Oguri M., Takada M., Umetsu K., Broadhurst T., 2005, ApJ, 632, 841
Oguri M., Bayliss M. B., Dahle H., Sharon K., Gladders M. D., Natarajan P., Hennawi J. F., Koester B. P., 2012, MNRAS, 420, 3213
Oguri M. et al., 2013, MNRAS, 429, 482
Okabe N., Umetsu K., 2008, PASJ, 60, 345
Okabe N., Takada M., Umetsu K., Futamase T., Smith G. P., 2010, PASJ, 62, 811
Okabe N., Bourdin H., Mazzotta P., Maurogordato S., 2011, ApJ, 741, 116
Okabe N., Smith G. P., Umetsu K., Takada M., Futamase T., 2013, preprint (arXiv:1302.2728)
Okabe N., Futamase T., Kajisawa M., Kuroshima R., 2014a, ApJ, 784, 90
Okabe N. et al., 2014b, preprint (arXiv:1406.3451)
Paulin-Henriksson S., Antonuccio-Delogu V., Haines C. P., Radovich M., Mercurio A., Becciani U., 2007, A&A, 467, 427
Pedersen K., Dahle H., 2007, ApJ, 667, 26
Piffaretti R., Arnaud M., Pratt G. W., Pointecouteau E., Melin J.-B., 2011, A&A, 534, A109
Planck Collaboration et al., 2014, A&A, 571, A20
Postman M. et al., 2012, ApJS, 199, 25
Prada F., Klypin A. A., Cuesta A. J., Betancort-Rijo J. E., Primack J., 2012, MNRAS, 423, 3018
Pratt G. W., Croston J. H., Arnaud M., Böhringer H., 2009, A&A, 498, 361
Radovich M., Puddu E., Romano A., Grado A., Getman F., 2008, A&A, 487, 55
Rasia E. et al., 2012, New J. Phys., 14, 055018
Reichardt C. L. et al., 2013, ApJ, 763, 127
Rines K., Diaferio A., 2006, AJ, 132, 1275
Romano A. et al., 2010, A&A, 514, A88
Rozo E., Rykoff E. S., Bartlett J. G., Evrard A., 2014, MNRAS, 438, 49
Schirmer M., Suyu S., Schrabback T., Hildebrandt H., Erben T., Halkola A., 2010, A&A, 514, A60
Schirmer M., Hildebrandt H., Kuijken K., Erben T., 2011, A&A, 532, A57
Sereno M., 2002, A&A, 393, 757
Sereno M., 2007, MNRAS, 380, 1207
Sereno M., Covone G., 2013, MNRAS, 434, 878
Sereno M., Ettori S., 2015a, MNRAS, 450, 3633 (CoMaLit-I)
Sereno M., Ettori S., 2015b, MNRAS, 450, 3675 (CoMaLit-IV)
Sereno M., Umetsu K., 2011, MNRAS, 416, 3187
Sereno M., Zitrin A., 2012, MNRAS, 419, 3280
Sereno M., Jetzer P., Lubini M., 2010, MNRAS, 403, 2077
Sereno M., Ettori S., Umetsu K., Baldi A., 2013, MNRAS, 428, 2241
Sereno M., Ettori S., Moscardini L., 2015, MNRAS, 450, 3649 (CoMaLit-II)
Sereno M., Giocoli C., Ettori S., Moscardini L., 2015, MNRAS, 449, 2024
Shan H. et al., 2012, ApJ, 748, 56
Smail I., Ellis R. S., Dressler A., Couch W. J., Oemler A., Sharples R. M., Butcher H., 1997, ApJ, 479, 70
Tinker J., Kravtsov A. V., Klypin A., Abazajian K., Warren M., Yepes G., Gottlöber S., Holz D. E., 2008, ApJ, 688, 709
Turner E. L., Ostriker J. P., Gott J. R., III, 1984, ApJ, 284, 1
Umetsu K. et al., 2009, ApJ, 694, 1643
Umetsu K., Broadhurst T., Zitrin A., Medezinski E., Hsu L.-Y., 2011, ApJ, 729, 127
Umetsu K. et al., 2014, ApJ, 795, 163
Voit G. M., 2005, Rev. Modern Phys., 77, 207
von der Linden A. et al., 2014, MNRAS, 439, 2
Watanabe E. et al., 2011, PASJ, 63, 357
Wold M., Lacy M., Dahle H., Lilje P. B., Ridgway S. E., 2002, MNRAS, 335, 1017
Wright C. O., Brainerd T. G., 2000, ApJ, 534, 34

SUPPORTING INFORMATION

Additional Supporting Information may be found in the online version of this article:

LC2_ReadMe.txt
LC2-all_v1.0.dat
LC2-single_v1.0.dat
LC2-substructure_v1.0.dat
(http://mnras.oxfordjournals.org/lookup/suppl/doi:10.1093/mnras/stu2505/-/DC1).

Please note: Oxford University Press are not responsible for the content or functionality of any supporting materials supplied by the authors. Any queries (other than missing material) should be directed to the corresponding author for the paper.

This paper has been typeset from a TEX/LATEX file prepared by the author.